ЖУРНАЛ СТРУКТУРНОЙ ХИМИИ

2015. Том 56, № 8 *Декабрь* *С. 1537 – 1544*

UDC 541.49:546.76:541.67

THEORETICAL STUDY OF SOLVENT AND SUBSTITUENT EFFECTS ON THE STRUCTURE, ^{14}N NQR AND ELECTRONIC SPECTRA OF [$Cr(CO)_5$py]

M.Z. Fashami[1], R. Ghiasi[2], Hoda Pasdar[3]

[1]*Department of Chemistry, Kerman Branch, Islamic Azad University, Kerman, Iran*
[2]*Department of Chemistry, East Tehran Branch, Islamic Azad University, Qiam Dasht, Tehran, Iran*
E-mail: rezaghiasi1353@yahoo.com
[3]*Faculty of Chemistry, North Tehran Branch, Islamic Azad University, Tehran, Iran*

Received October, 22, 2014

The structure, ^{14}N NQR parameters, electronic spectra, and hyperplarizability of [$Cr(CO)_5$py] in seven different solvents were theoretically computed with MPW1PW91 method based on Polarizable Continuum Model (PCM). The substituent effects in *para*- substituted $Cr(CO)_5$— pyridine complexes have been evaluated. The results indicate that both polarity of solvents and the substituents have played a significant role on the structures and properties of complexes. The study also shows that the structural and solvent modification change the NLO properties.

DOI: 10.15372/JSC20150804

K e y w o r d s: [$Cr(CO)_5$py] complexes, substituent effect, solvent effect, ^{14}N NQR parameters.

INTRODUCTION

The [$M(CO)_5$py] (M = Cr, Mo, W) complexes have been well-known for extended period of time [1]. Furthermore, group 6 metal carbonyl complexes of substituted pyridines are also synthesized [2]. [$M(CO)_5$(L)] complexes with L = 4-methylpyridine or 4-phenylpyridine have been isolated [3—5]. 2-Substituted pyridine derivatives, for instance, 2-cyanopyridine and 2-phenylpyridine also form complexes of the [$M(CO)_5$L] type [6]. The catalytic properties [7], photochemistry [8], and non-linear optical properties [9] of these compounds have been explored. Pyridine (py) is a σ-donor ligand with a slight π-accepting ability, therefore, the M—N bond in these low valent metal complexes is very weak. For that reason, the [$M(CO)_5$(py)] complexes have an increased lability toward ligand substitution. Also, the structure and properties of [$M(CO)_5$L] derivatives are investigated by means of computational methods [10, 11]. For instance, the substituent effects in *para* substituted $Cr(CO)_5$— pyridine complexes have been evaluated on the basis of DFT quantum-chemical calculations [10].

In the present paper we report the solvent and substituent effects on the structure, ^{14}N NQR and electronic spectra of [$Cr(CO)_5$(pyridine)], using quantum chemical calculations. We also explain the structure-property relationships.

COMPUTATIONAL METHODS

All calculations were carried out with the Gaussian 03 program suite [12]. The systems with C, B, O, N, Cl, F and H are described by the standard 6-311G(*d,p*) basis set [13—16]. For chromium standard LANL2DZ basis set [17—19] was used, and chromium was described by effective core potential (ECP) of Wadt and Hay pseudopotential [17] with a doublet-ξ valance using the LANL2DZ. Geometry optimization was performed with Modified Perdew-Wang Exchange and Correlation (MPW1PW91) [20]. The results of calculations for transition metal complexes show that MPW1PW91

functional gives better results than B3LYP [21—24]. A vibrational analysis was performed at each stationary point found, to confirm its identity as real energy minimum.

Using this method, the geometry was re-optimized and the UV/Vis spectrum was calculated by DFT/TD-DFT with the same functionals and basis sets [25]. The 10 lowest excitation energies were computed.

Then the geometry of each species in solvents with different dielectric constants was calculated at the same level with the polarized continuum model (PCM) [26].

The electrostatic interaction of a nuclear electric quadrupole moment and the electron charge cloud surrounding the nucleus can give rise to the observation of pure Nuclear Quadrupole Resonance (NQR) [27]. The Hamiltonian of this interaction for a nucleus of spin I is given [28]:

$$H_Q = \frac{e^2 Q q_{zz}}{4I(2I-1)}[3I_z^2 - I^2 + \frac{\eta}{2}(I_+^2 + I_-^2)], \tag{1}$$

where all Is in the denominator are scalar values while all Is in the square brackets are operators [29]. Quantum chemical calculations yield principal components of the EFG tensor, q_{ii}, in atomic units (1 au = 9.717365×10^2 Vm^{-2}) [8], with $|q_{zz}| \geq |q_{yy}| \geq |q_{xx}|$. q_{xx}, q_{yy} and q_{zz} are the components of EFG in the directions of x, y and z, respectively. The calculated q_{ii} values were used to obtain the nuclear quadrupole coupling constants, χ_{ii}:

$$\chi_{ii}(MHz) = \frac{e^2 Q q_{ii}}{h}, \qquad i = x, y, z, \tag{2}$$

where Q is the nuclear quadrupole moment of the ^{14}N nucleus. The standard values of quadrupole moment, Q, reported by Pyykkö [30] were used in Eq. (1), $Q(^{14}\text{N}) = 20.44$ mb. Often the NQR parameters experimentally are reported as the nuclear quadrupole coupling constant, and have the unit of frequency:

$$QCC = \chi(\text{MHz}) = \frac{e^2 Q q_{zz}}{h}. \tag{3}$$

Asymmetry parameters (η_Q) are defined as:

$$\eta_Q = \left|\frac{(q_{yy} - q_{xx}}{q_{zz}}\right|; \qquad 0 \leq \eta_Q \leq 1; \tag{4}$$

since it measures the deviation of the field gradient tensor from axial symmetry.

For a nucleus of unit spin (such as ^{14}N), we have three energy levels, so we get three nuclear quadrupole resonance frequencies [28]:

$$\upsilon_+ = \frac{3}{4}\chi_{zz}(1 + \frac{\eta}{3}), \tag{5}$$

$$\upsilon_- = \frac{3}{4}\chi_{zz}(1 - \frac{\eta}{3}), \tag{6}$$

$$\upsilon_0 = \frac{3}{4}\chi_{zz}\eta. \tag{7}$$

The quadrupole coupling constant (χ_{zz}) and asymmetry parameter (η) are usually calculated from the nuclear quadrupole frequencies as follows:

$$\chi_{zz} = \frac{2(\upsilon_+ + \upsilon_-)}{3}, \tag{8}$$

$$\eta = \frac{3(\upsilon_+ - \upsilon_-)}{(\upsilon_+ + \upsilon_-)}. \tag{9}$$

Geometries were optimized at this level of theory without any symmetry constraints followed by the calculations of the first order hyperpolarizabilities. The total static first hyperpolarizability β was obtained from the relation:

$$\beta_{\text{tot}} = \sqrt{\beta_x^2 + \beta_y^2 + \beta_z^2}$$

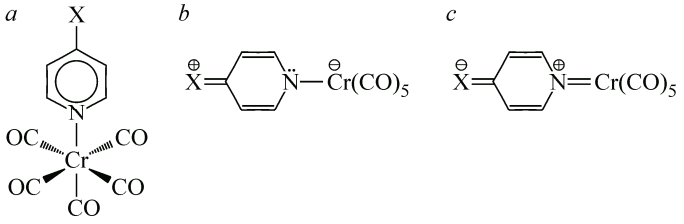

Fig. 1. Para-substituted [$Cr(CO)_5$py] (*a*), and resonance forms for electron donor (*b*), and electron withdrawing substituents (*c*)

upon calculating the individual static components

$$\beta_i = \beta_{iii} + \frac{1}{3}\sum_{i \neq j}(\beta_{ijj} + \beta_{jij} + \beta_{jji}).$$

Due to the Kleinman symmetry [31]:

$$\beta_{xyy} = \beta_{yxy} = \beta_{yyx}; \quad \beta_{yyz} = \beta_{yzy} = \beta_{zyy}, \ldots$$

one finally obtains the equation that has been employed:

$$\beta_{tot} = \sqrt{(\beta_{xxx} + \beta_{xyy} + \beta_{xzz})^2 + (\beta_{yyy} + \beta_{yzz} + \beta_{yxx})^2 + (\beta_{zzz} + \beta_{zxx} + \beta_{zyy})^2}\ .$$

RESULTS AND DISCUSSION

Energy. Fig. 1 shows the molecular structure of *para*-substitued [$Cr(CO)_5$py] complexes. The energies of the [$Cr(CO)_5$py] complexes in the gas phase and in different media calculated by using the PCM model are listed in Table 1. E_T is the total energy and ΔE_{solv} is the stabilization energy by solvents, defined as relative energy of the title compound in a solvent to that in the gas phase.

From Table 1, we can see that the calculated energy is dependent on the size of the dielectric constant of solvents. In the PCM model, the energies E_T decrease with the increasing dielectric constants.

Table 1

Absolute energy (*E*, Hartree), *dipole moment* (μ, Debye) *values*, *selected structural parameters* (Å), *and solvent stabilization energies* (ΔE_{solv}, kcal/mol) *values of* [$Cr(CO)_5$py] *in different media*, *calculated by* PCM *model*, *and absolute energy* (*E*, Hartree), *dipole moment* (μ, Debye) *values*, *selected structural parameters* (Å) *of* [$Cr(CO)_5$py] *and* [$Cr(CO)_5$(p-XC_5H_4N)] *complexes*

Solvent	ε	E_T	ΔE_{solv}	μ	*d*(Cr—N)	*d*(Cr—CO_{cis})	*d*(Cr—CO_{trans})
Gas	—	–901.3280	—	6.89	2.17625	1.88937	1.84172
Chloroform	4.9	–901.3346	–4.14	8.12	2.17560	1.88829	1.83369
ChloroBenzene	5.621	–901.3351	–4.41	8.20	2.17591	1.88841	1.83370
Aniline	6.89	–901.3354	–4.64	8.26	2.17585	1.88838	1.83324
THF	7.58	–901.3356	–4.72	8.29	2.17584	1.88838	1.83308
MethyleneChloride	8.93	–901.3358	–4.90	8.34	2.17580	1.88836	1.83271
Quinoline	9.03	–901.3359	–4.92	8.35	2.17576	1.88835	1.83237
Isoquinoline	10.43	–901.3361	–5.07	8.39	2.17579	1.88836	1.83267
X							
F	—	–1000.5690	—	5.45	2.18146	1.88956	1.84163
Cl	—	–1360.9560	—	5.30	2.17638	1.88979	1.84251
Me	—	–940.6490	—	7.71	2.17610	1.88901	1.84105
NH_2	—	–956.6973	—	9.69	2.17931	1.88796	1.83933
OH	—	–976.5577	—	7.63	2.18109	1.88828	1.84040
NO_2	—	–1105.8244	—	2.01	2.16340	1.89130	1.84639
CN	—	–993.5575	—	2.18	2.16536	1.89090	1.84560
CHO	—	–1014.6464	—	4.48	2.16383	1.89013	1.84499
COOH	—	–1089.9072	—	5.92	2.16663	1.89064	1.84410

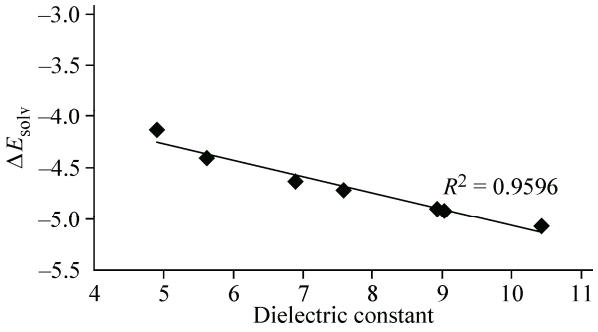

Fig. 2. Correlation between dielectric constants and ΔE_{solv} in $[Cr(CO)_5py]$

As seen from ΔE_{solv} values, the stability of $[Cr(CO)_5py]$ increases in more polar solvents. This is because a dipole in the molecule will induce a dipole in the medium, and the electric field applied to the solute by the solvent (reaction) dipole will in turn interact with the molecular dipole to lead to net stabilization. This suggests that a $[Cr(CO)_5py]$ complex has more stability in a polar solvent rather than in the gas phase. There is a good correlation between dielectric constants and ΔE_{solv} (Fig. 2).

Dipole moment. Dipole moments in $[Cr(CO)_5py]$ complex in gas phase and in different media calculated by the PCM model are listed in Table 1. These values show the solvent effect on the stabilization energy runs parallel with the dipole moment of the solute. A good linear relationship between the solvent stabilization energies and the dipole moments of $[Cr(CO)_5py]$ in the set of solvents is shown in Fig. 3, *a*, and the correlation coefficient is –0.999. The larger is the dipole moment of solute, the higher is the stabilization energy in a more polar solvent. There is also a good correlation between dipole moment and dielectric constants (Fig. 3, *b*).

Bond distances. Selected bond distances in $[Cr(CO)_5py]$ complex are given in Table 1. It is well-known that the solvent polarity influences both the structure and properties of conjugated organic molecules and metal complexes [32—34]. The structural data for the optimized structures of $[Cr(CO)_5py]$ complex in the five studied solvents are compiled in Table 1. The results show that the

T a b l e 2

^{14}N NQR *parameters of* $[Cr(CO)_5py]$ *in different media*

Solvent	q_{xx}, a.u.	q_{yy}, a.u.	q_{zz}, a.u.	$(e^2Q/h)q_{xx}$	$(e^2Q/h)q_{yy}$	$(e^2Q/h)q_{zz}$	η	υ_+	υ_-	υ_0
Gas	–0.24925	–0.4673	0.716552	–1.197	–2.244	3.442	0.304	2.843	2.319	0.524
Chloroform	–0.24705	–0.43466	0.681709	–1.187	–2.088	3.274	0.275	2.681	2.230	0.451
ChloroBenzene	–0.24574	–0.43349	0.679222	–1.180	–2.082	3.262	0.276	2.672	2.221	0.451
Aniline	–0.24555	–0.43185	0.677396	–1.179	–2.074	3.254	0.275	2.664	2.216	0.447
THF	–0.24548	–0.43127	0.676754	–1.179	–2.071	3.250	0.275	2.661	2.215	0.446
MethyleneChloride	–0.24534	–0.43001	0.675351	–1.178	–2.065	3.244	0.273	2.655	2.211	0.443
Quinoline	–0.24532	–0.42985	0.675175	–1.178	–2.065	3.243	0.273	2.654	2.211	0.443
Isoquinoline	–0.2452	–0.42882	0.674025	–1.178	–2.060	3.237	0.272	2.648	2.208	0.441

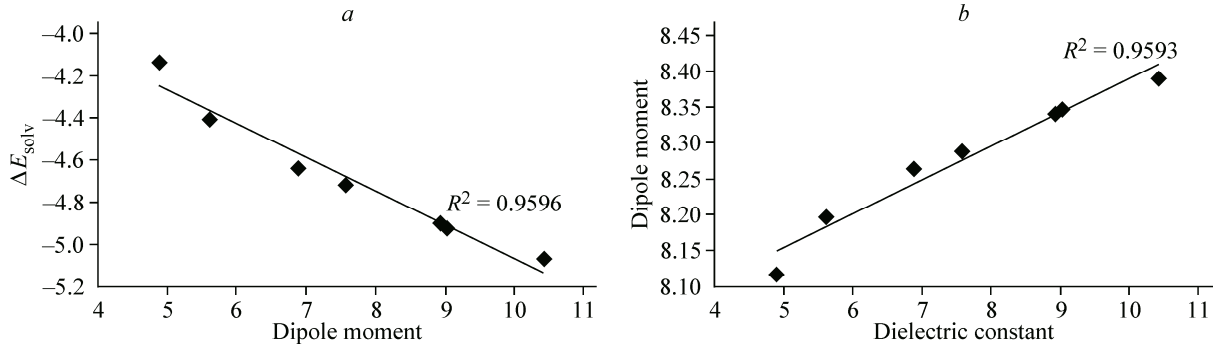

Fig. 3. Correlation between dipole moment and ΔE_{solv} (*a*), and dielectric constants and dipole moments in $[Cr(CO)_5py]$ (*b*)

Table 3

^{14}N NQR *parameters of para-substituted pyridine and* [Cr(CO)$_5$py] *in gas phase*

X	σ_p	σ^+	q_{xx}, a.u.	q_{yy}, a.u.	q_{zz}, a.u.	$(e^2Q/h)q_{xx}$	$(e^2Q/h)q_{yy}$	$(e^2Q/h)q_{zz}$	η	υ_+	υ_-	υ_0
					py							
H	0.00		–0.352559	–0.776422	1.128981	–1.693	–3.729	5.422	0.375	4.576	3.558	1.018
F	0.06		–0.384322	–0.707139	1.091461	–1.846	–3.396	5.242	0.296	4.319	3.544	0.775
Cl	0.23		–0.384322	–0.707139	1.091461	–1.846	–3.396	5.242	0.296	4.319	3.544	0.775
Me	–0.17		–0.360486	–0.740388	1.100874	–1.731	–3.556	5.287	0.345	4.422	3.509	0.912
NH_2	–0.66		–0.410971	–0.605442	1.016412	–1.974	–2.908	4.882	0.191	3.895	3.428	0.467
OH	–0.37		–0.399079	–0.649848	1.048927	–1.917	–3.121	5.038	0.239	4.080	3.477	0.602
NO_2	0.78		–0.410971	–0.605442	1.016412	–1.974	–2.908	4.882	0.191	3.895	3.428	0.467
CN	0.66		–0.340951	–0.817990	1.158941	–1.638	–3.929	5.566	0.412	4.748	3.602	1.146
CHO	0.42		–0.337010	–0.833739	1.170749	–1.619	–4.004	5.623	0.424	4.814	3.621	1.193
COOH	0.45		–0.334520	–0.830716	1.165236	–1.607	–3.990	5.597	0.426	4.793	3.602	1.192
					[Cr(CO)$_5$py]							
H	0.00	0	–0.24925	–0.4673	0.716552	–1.197	–2.244	3.442	0.304	2.843	2.319	0.524
F	0.06	–0.07	–0.28925	–0.40204	0.691292	–1.389	–1.931	3.320	0.163	2.626	2.355	0.271
Cl	0.23	0.11	–0.27057	–0.43688	0.707445	–1.300	–2.098	3.398	0.235	2.748	2.349	0.399
Me	–0.17	–0.31	–0.26005	–0.42529	0.685339	–1.249	–2.043	3.292	0.241	2.667	2.270	0.397
NH_2	–0.66	–1.3	–0.26359	–0.32607	0.589658	–1.266	–1.566	2.832	0.106	2.199	2.049	0.150
OH	–0.37	–0.92	–0.30713	–0.333	0.640121	–1.475	–1.599	3.075	0.040	2.337	2.275	0.062
NO_2	0.78	0.79	–0.23801	–0.53162	0.769621	–1.143	–2.553	3.696	0.382	3.125	2.420	0.705
CN	0.66	0.66	–0.24176	–0.51096	0.752718	–1.161	–2.454	3.615	0.358	3.035	2.388	0.646
CHO	0.42	0.73	–0.23408	–0.51907	0.753147	–1.124	–2.493	3.617	0.378	3.055	2.371	0.684
COOH	0.45	0.42	–0.23196	–0.5165	0.748459	–1.114	–2.481	3.595	0.380	3.038	2.354	0.683

structural parameters are changed by the polarity of the surrounding media. These values indicate shortening of Cr—N, Cr—C_{cis}, and Cr—Cr_{trans} bonds in this set of solvents rather than gas phase.

As is seen from Table 1, the Cr—N bond distances are shorter for electron withdrawing substituents. This shortening arises from an increase in the π-accepting force of a pyridine ligand. See resonance form (*c*) in Fig. 1.

^{14}N-NQR parameters. The distortion of the charge distributions around nitrogen atom has been investigated, and interpreted by EFGs. The EFG around a nitrogen nucleus is symmetric in N_2, and calculated values of NQR parameters for N_2 molecule are $\eta_Q = 0$ and $\nu_Q^{cal} = 4.258$ MHz. The calculated NQR frequencies of nitrogen atom in [Cr(CO)$_5$py] in the gas phase and different solvents are listed in Table 3. These values show that χ_{zz} and η values decrease from the gas phase to the solution. On the other hand, υ_+, υ_-, and υ_0 frequencies are sensitive to solvents. Fig. 4 presents good linear relationships between these values and dielectric constants. The corresponding equations are:

$$\upsilon_+ = -0.005\,\varepsilon + 2.705, \quad \upsilon_- = -0.003\,\varepsilon + 2.243, \quad \upsilon_0 = -0.002\,\varepsilon + 0.461.$$

Electronic spectra. The wavelength, oscillator strengths and the contribution to the maximum electronic transitions of *para*-substituted [Cr(CO)$_5$py] complexes are given in Table 4 in gas phase. These transitions are attributed to the HOMO → LUMO transition. The plot of frontier orbitals is presented in Fig. 5. The largest contribution to HOMO arises from Cr(CO)$_5$ fragment and pyridine ligand, and LUMO is located on the pyridine ligand. Table 4 shows that the introduction of an electron withdrawing groups (EWG) decreases the frontier orbital energy. On the other hand, introduction of the electron-accepting group increases the HOMO-LUMO gap. Therefore, λ_{max} values of withdrawing electron groups are more than donor electron groups.

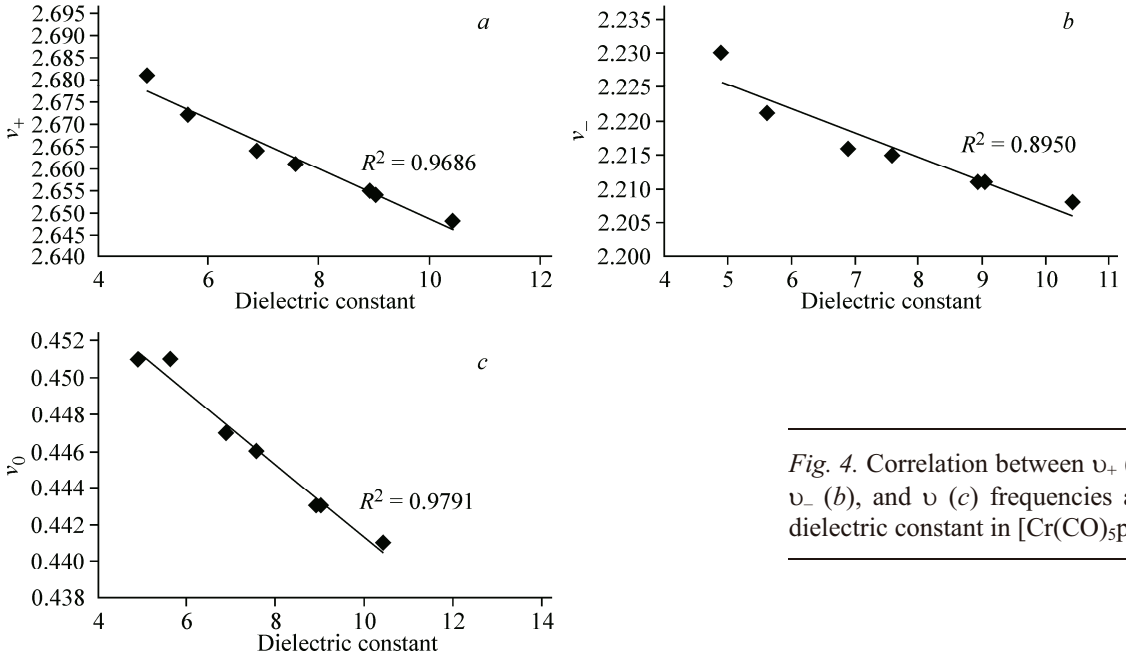

Fig. 4. Correlation between υ_+ (*a*), υ_- (*b*), and υ (*c*) frequencies and dielectric constant in $[Cr(CO)_5py]$

T a b l e 4

Frontier orbital energies, HOMO-LUMO *gap* (eV), *wavelength* (nm), *oscillator strengths*, *the composition of the maximum electronic transitions*, *and hyperpolarizability* (esu) *of para-substituted* $[Cr(CO)_5(XC_5H_4N)]$ *complexes in gas phase*

X	*E*(HOMO)	*E*(LUMO)	Δ*E*	Transition	λ_{max}	*f*	$\beta_{tot}\times10^{-30}$
H	–0.22977	–0.06740	4.42	HOMO → LUMO	349.40	0.1010	12.57
F	–0.23285	–0.06537	4.56	HOMO → LUMO	336.73	0.0922	8.75
Cl	–0.23385	–0.07704	4.27	HOMO → LUMO	362.27	0.1290	14.40
Me	–0.22687	–0.06098	4.51	HOMO → LUMO	337.76	0.0635	12.04
NH_2	–0.21931	–0.03977	4.89	HOMO → LUMO	306.54	0.1046	3.47
OH	–0.22637	–0.05082	4.78	HOMO → LUMO	317.79	0.1011	6.09
NO_2	–0.24312	–0.13067	3.06	HOMO → LUMO	505.14	0.1483	72.31
CN	–0.24139	–0.11040	3.56	HOMO → LUMO	436.96	0.1633	42.74
CHO	–0.23704	–0.11401	3.35	HOMO → LUMO	461.69	0.1564	55.44
COOH	–0.23462	–0.10184	3.61	HOMO → LUMO	429.05	0.1520	41.94

The calculated wavelengths, oscillator strengths and the composition of the maximum electronic transitions values of $[Cr(CO)_5py]$ in different media are compiled in Table 5. The solvation effects indicate that as the dielectric constant increases, a blue shift is observed. On the other hand, the comparison of $\boldsymbol{\lambda_{max}}$ values in gas and solution phases alsoshows a blue shift to occur in solution phase. Fig. 6 indicates a good correlation between dielectric constant and $\boldsymbol{\lambda_{max}}$ values.

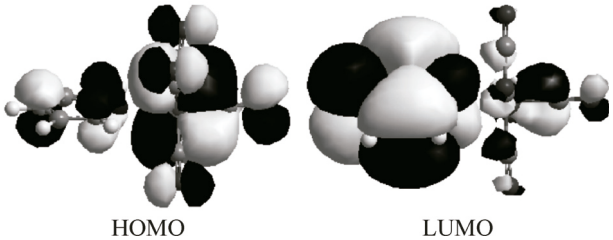

Fig. 5. The plot of frontier orbitals for $[Cr(CO)_5py]$

Table 5

The wavelength, oscillator strengths, the composition of the maximum electronic transitions, and hyperpolarizability values of $[Cr(CO)_5py]$

Solvent	λ_{max}	f	$\beta_{tot}\times10^{30}$
Gas	349.40	0.1010	12.57
Chloroform	320.74	0.1204	13.03
ChloroBenzene	319.22	0.1227	13.02
Aniline	318.02	0.1244	13.04
THF	317.09	0.1166	13.04
MethyleneChloride	316.13	0.1168	13.06
Quinoline	314.40	0.0923	13.06
Isoquinoline	313.61	0.0917	13.07

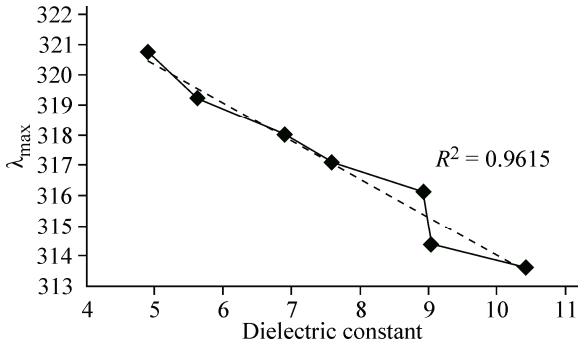

Fig. 6. Linear correlation between dielectric constant and λ_{max} values in $[Cr(CO)_5py]$

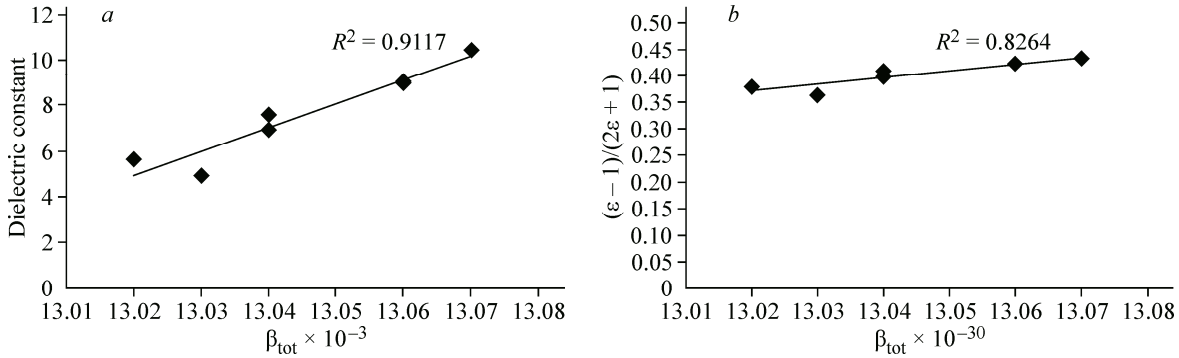

Fig. 7. Dependence of the first hyperpolarizabilities on the dielectric constant (*a*), and Onsager function (*b*) in $[Cr(CO)_5py]$

Fig. 8. Resonance forms of X = NO_2 in [*para*-$XC_5H_4Cr(CO)_5$] complex

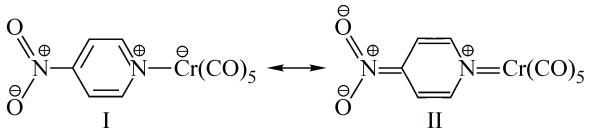

Hyperpolarizability. The solvent polarity plays an important role on the first hyperpolarizabilities in dipolar molecules. The β_{tot} values of $[Cr(CO)_5py]$ in various solvents have been gathered in Table 5. These values indicate that β_{tot} values increase on going from vacuum into solution. The dependence of the first hyperpolarizability both on the dielectric constant and the Onsager function has been investigated [35]. Fig. 7 is typical for a dipolar reaction field interaction in the solvation process [35—38]. Therefore, the electronic reorganization in solution for $[Cr(CO)_5py]$ exercises a significant effect on the first hyperpolarizabilities.

The calculated first static hyperpolarizabilities for *para*-substituted $[Cr(CO)_5py]$ complexes are shown in Table 4. These values indicate that the most β_{tot} values are highest in the presence of EWG. For X = NO_2 the value is the highest, because of the greater charge separation in the dominate resonance form (I) in this molecule (Fig. 8).

CONCLUSIONS

Theoretically investigation of solvent effect on the structure, ^{14}N NQR parameters, electronic spectra, and hyperplarizability of $[Cr(CO)_5py]$ and the substituent effect in *para* substituted $[Cr(CO)_5$—pyridine] complexes show that:

1. The Cr—N, Cr—C_{cis}, and Cr—Cr_{trans} bond lengths decrease on going into solution.

2. The χ_{zz} and η values of ^{14}N NQR parameters decrease on going from the gas phase into the solution.

3. The wavelength decreases as the dielectric constant increases. There is a blue shift on going into solution.

4. The hyperpolarizability values are higher in vacuum. The β_{tot} values increase in the presence of WEG.

REFERENCES

1. *Dennenberg R.J., Darensbourg D.J.* // Inorg. Chem. – 1972. – **11**. – P. 72.
2. *Weiner M.A., Gin A., Lattman M.* // Inorg. Chim. Acta. – 1977. – **24**. – P. 235.
3. *Kolodziej R.M., Lees A.J.* // Organometallics. – 1986. – **5**. – P. 450.
4. *Creaven B.S., Howie R.A., Long C.* // Acta Crystallogr., Sect. C. – 2001. – **57**. – P. 385.
5. *Boxhoorn G.S., Stufkens D.J., Van der Coolwijk P.J.M., Hezemans A.M.F.* // Inorg. Chem. – 1981. – **20**. – P. 2778.
6. *Creaven B.S., Howie R.A., Long C.* // Acta Crystallogr., Sect. C. – 2000. – **56**. – P. 181.
7. *Solomon E.I., Jones P.M., May J.A.* // Chem. Rev. – 1993. – **93**. – P. 2623.
8. *Wrighton M.* // Chem. Rev. – 1974. – **74**. – P. 401.
9. *Bruschi M., Fantucci P., Pizzotti M.* // J. Phys. Chem. A. – 2005. – **109**. – P. 9637.
10. *Palusiak M.* // J. Organomet. Chem. – 2007. – **692**. – P. 3866 – 3873.
11. *Ehlers A.W., Dapprich S., Vyboishchikov S.F., Frenking G.* // Organometallics. – 1996. – **15**. – P. 105.
12. *Frisch M.J., Trucks G.W., Schlegel H.B., Scuseria G.E., Robb M.A., Cheeseman J.R., Montgomery J.A. Jr., Vreven T., Kudin K.N., Burant J.C., Millam J.M., Iyengar S.S., Tomasi J., Barone V., Mennucci B., Cossi M., Scalmani G., Rega N., Petersson G.A., Nakatsuji H., Hada M., Ehara M., Toyota K., Fukuda R., Hasegawa J., Ishida M., Nakajima T., Honda Y., Kitao O., Nakai H., Klene M., Li X., Knox J.E., Hratchian H.P., Cross J.B., Adamo C., Jaramillo J., Gomperts R., Stratmann R.E., Yazyev O., Austin A.J., Cammi R., Pomelli C., Ochterski J.W., Ayala P.Y., Morokuma K., Voth G.A., Salvador P., Dannenberg J.J., Zakrzewski V.G., Dapprich S., Daniels A.D., Strain M.C., Farkas O., Malick D.K., Rabuck A.D., Raghavachari K., Foresman J.B., Ortiz J.V., Cui Q., Baboul A.G., Clifford S., Cioslowski J., Stefanov B.B., Liu G., Liashenko A., Piskorz P., Komaromi I., Martin R.L., Fox D.J., Keith T., Al-Laham M.A., Peng C.Y., Nanayakkara A., Challacombe M., Gill P.M.W., Johnson B., Chen W., Wong M.W., Gonzalez C., Pople J.A*. In: Gaussian, Inc., Pittsburgh, PA, 2003.
13. *Krishnan R., Binkley J.S., Seeger R., Pople J.A.* // J. Chem. Phys. – 1980. – **72**. – P. 650 – 654.
14. *Wachters A.J.H.* // J. Chem. Phys. – 1970. – **52**. – P. 1033.
15. *Hay P.J.* // J. Chem. Phys. – 1977. – **66**. – P. 4377 – 4384.
16. *McLean A.D., Chandler G.S.* // J. Chem. Phys. – 1980. – **72**. – P. 5639 – 5648.
17. *Hay P.J., Wadt W.R.* // J. Chem. Phys. – 1985. – **82**. – P. 299 – 310.
18. *Hay P.J., Wadt W.R.* // J. Chem. Phys. – 1985. – **82**. – P. 284 – 298.
19. *Schaefer A., Horn H., Ahlrichs R.* // J. Chem. Phys. – 1992. – **97**. – P. 2571 – 2577.
20. *Adamo B., Barone V.* // J. Chem. Phys. – 1998. – **108**. – P. 664.
21. *Porembski J.P.C.A.M., Weisshaar J.C.* // J. Phys. Chem. A. – 2001. – **105**. – P. 4851.
22. *Porembski M., Weisshaar J.C.* // J. Phys. Chem. A. – 2001. – **105**. – P. 6655 – 6667.
23. *Zhang Y., Guo Z., You X.-Z.* // J. Am. Chem. Soc. – 2001. – **123**. – P. 9378 – 9387.
24. *Dunbar R.C.* // J. Phys. Chem. A. – 2002. – **106**. – P. 7328 – 7337.
25. *Runge E., Gross E.K.U.* // Phys. Rev. Lett. – 1984. – **52**. – P. 997 – 1000.
26. *Tomasi J., Mennucci B., Cammi R.* // Chem. Rev. – 2005. – **105**. – P. 2999 – 3093.
27. *Graybeal J.D*. Molecular Spectroscopy. – McGraw-Hill, 1988.
28. *Seliger J*. Nuclear Quadrupole Resonance, Theory — Encyclopedia of Spectroscopy and Spectrometry. – Academic Press, 2000.
29. *Slichter C.P*. Principles of Magnetic Resonance. – 3rd ed. – Heidelberg: Springer-Verlag, 1990.
30. *Tokman M., Sundholm D., Pyykkö P., Olsen J.* // Chem. Phys. Lett. – 1997. – **265**. – P. 60.
31. *Keleiman D.A.* // Phys. Rev. – 1962. – **126**. – P. 1977.
32. *Mendes P.J., Silva T.J.L., Carvalho A.J.P., Ramalho J.P.P.* // J. Mol. Struct.: THEOCHEM. – 2010. – **946**. – P. 33 – 42.
33. *Chen L.M., Chen J.C., Luo H. et al.* // J. Theor. Comput. Chem. – 2011. – **10**. – P. 581 – 604.
34. *Cao X., Liu C., Liu Y.* // J. Theor. Comput. Chem. – 2012. – **11**. – P. 573 – 586.
35. *Onsager L.* // J. Am. Chem. Soc. – 1936. – **58**. – P. 1486.
36. *Clays K., Persoons A.* // Phys. Rev. Lett. – 1991. – **66**. – P. 2980.
37. *Lee H., An S.-Y., Cho M.* // J. Phys. Chem. B. – 1999. – **103**. – P. 4992.
38. *Ray P.C., Leszczynski J.* // Chem. Phys. Lett. – 2004. – **399**. – P. 162.